DESY 11-123 ISSN 0418-9833
July 2011

Search for First Generation Leptoquarks in ep Collisions at HERA

H1 Collaboration

Abstract

A search for first generation scalar and vector leptoquarks produced in ep collisions is performed by the H1 experiment at HERA. The full H1 data sample is used in the analysis, corresponding to an integrated luminosity of 446 pb^{-1}. No evidence for the production of leptoquarks is observed in final states with a large transverse momentum electron or with large missing transverse momentum, and constraints on leptoquark models are derived. For leptoquark couplings of electromagnetic strength $\lambda = 0.3$, first generation leptoquarks with masses up to 800 GeV are excluded at 95% confidence level.

Accepted by *Phys. Lett.* **B**

F.D. Aaron[5,48], C. Alexa[5], V. Andreev[25], S. Backovic[30], A. Baghdasaryan[38], S. Baghdasaryan[38], E. Barrelet[29], W. Bartel[11], K. Begzsuren[35], A. Belousov[25], P. Belov[11], J.C. Bizot[27], V. Boudry[28], I. Bozovic-Jelisavcic[2], J. Bracinik[3], G. Brandt[11], M. Brinkmann[11], V. Brisson[27], D. Britzger[11], D. Bruncko[16], A. Bunyatyan[13,38], G. Buschhorn[26,†], L. Bystritskaya[24], A.J. Campbell[11], K.B. Cantun Avila[22], F. Ceccopieri[4], K. Cerny[32], V. Cerny[16,47], V. Chekelian[26], J.G. Contreras[22], J.A. Coughlan[6], J. Cvach[31], J.B. Dainton[18], K. Daum[37,43], B. Delcourt[27], J. Delvax[4], E.A. De Wolf[4], C. Diaconu[21], M. Dobre[12,50,51], V. Dodonov[13], A. Dossanov[26], A. Dubak[30,46], G. Eckerlin[11], S. Egli[36], A. Eliseev[25], E. Elsen[11], L. Favart[4], A. Fedotov[24], R. Felst[11], J. Feltesse[10], J. Ferencei[16], D.-J. Fischer[11], M. Fleischer[11], A. Fomenko[25], E. Gabathuler[18], J. Gayler[11], S. Ghazaryan[11], A. Glazov[11], L. Goerlich[7], N. Gogitidze[25], M. Gouzevitch[11,45], C. Grab[40], A. Grebenyuk[11], T. Greenshaw[18], B.R. Grell[11], G. Grindhammer[26], S. Habib[11], D. Haidt[11], C. Helebrant[11], R.C.W. Henderson[17], E. Hennekemper[15], H. Henschel[39], M. Herbst[15], G. Herrera[23], M. Hildebrandt[36], K.H. Hiller[39], D. Hoffmann[21], R. Horisberger[36], T. Hreus[4,44], F. Huber[14], M. Jacquet[27], X. Janssen[4], L. Jönsson[20], H. Jung[11,4,52], M. Kapichine[9], I.R. Kenyon[3], C. Kiesling[26], M. Klein[18], C. Kleinwort[11], T. Kluge[18], R. Kogler[11], P. Kostka[39], M. Kraemer[11], J. Kretzschmar[18], K. Krüger[15], M.P.J. Landon[19], W. Lange[39], G. Laštovička-Medin[30], P. Laycock[18], A. Lebedev[25], V. Lendermann[15], S. Levonian[11], K. Lipka[11,50], B. List[11], J. List[11], R. Lopez-Fernandez[23], V. Lubimov[24], A. Makankine[9], E. Malinovski[25], P. Marage[4], H.-U. Martyn[1], S.J. Maxfield[18], A. Mehta[18], A.B. Meyer[11], H. Meyer[37], J. Meyer[11], S. Mikocki[7], I. Milcewicz-Mika[7], F. Moreau[28], A. Morozov[9], J.V. Morris[6], M. Mudrinic[2], K. Müller[41], Th. Naumann[39], P.R. Newman[3], C. Niebuhr[11], D. Nikitin[9], G. Nowak[7], K. Nowak[11], J.E. Olsson[11], D. Ozerov[24], P. Pahl[11], V. Palichik[9], I. Panagoulias[l,11,42], M. Pandurovic[2], Th. Papadopoulou[l,11,42], C. Pascaud[27], G.D. Patel[18], E. Perez[10,45], A. Petrukhin[11], I. Picuric[30], S. Piec[11], H. Pirumov[14], D. Pitzl[11], R. Plačakytė[12], B. Pokorny[32], R. Polifka[32], B. Povh[13], V. Radescu[14], N. Raicevic[30], T. Ravdandorj[35], P. Reimer[31], E. Rizvi[19], P. Robmann[41], R. Roosen[4], A. Rostovtsev[24], M. Rotaru[5], J.E. Ruiz Tabasco[22], S. Rusakov[25], D. Šálek[32], D.P.C. Sankey[6], M. Sauter[14], E. Sauvan[21], S. Schmitt[11], L. Schoeffel[10], A. Schöning[14], H.-C. Schultz-Coulon[15], F. Sefkow[11], L.N. Shtarkov[25], S. Shushkevich[26], T. Sloan[17], I. Smiljanic[2], Y. Soloviev[25], P. Sopicki[7], D. South[11], V. Spaskov[9], A. Specka[28], Z. Staykova[4], M. Steder[11], B. Stella[33], G. Stoicea[5], U. Straumann[41], T. Sykora[4,32], P.D. Thompson[3], T.H. Tran[27], D. Traynor[19], P. Truöl[41], I. Tsakov[34], B. Tseepeldorj[35,49], J. Turnau[7], K. Urban[15], A. Valkárová[32], C. Vallée[21], P. Van Mechelen[4], Y. Vazdik[25], D. Wegener[8], E. Wünsch[11], J. Žáček[32], J. Zálešák[31], Z. Zhang[27], A. Zhokin[24], H. Zohrabyan[38], and F. Zomer[27]

[1] *I. Physikalisches Institut der RWTH, Aachen, Germany*
[2] *Vinca Institute of Nuclear Sciences, University of Belgrade, 1100 Belgrade, Serbia*
[3] *School of Physics and Astronomy, University of Birmingham, Birmingham, UK[b]*
[4] *Inter-University Institute for High Energies ULB-VUB, Brussels and Universiteit Antwerpen, Antwerpen, Belgium[c]*
[5] *National Institute for Physics and Nuclear Engineering (NIPNE) , Bucharest, Romania[m]*
[6] *Rutherford Appleton Laboratory, Chilton, Didcot, UK[b]*
[7] *Institute for Nuclear Physics, Cracow, Poland[d]*
[8] *Institut für Physik, TU Dortmund, Dortmund, Germany[a]*
[9] *Joint Institute for Nuclear Research, Dubna, Russia*

[10] *CEA, DSM/Irfu, CE-Saclay, Gif-sur-Yvette, France*
[11] *DESY, Hamburg, Germany*
[12] *Institut für Experimentalphysik, Universität Hamburg, Hamburg, Germany*[a]
[13] *Max-Planck-Institut für Kernphysik, Heidelberg, Germany*
[14] *Physikalisches Institut, Universität Heidelberg, Heidelberg, Germany*[a]
[15] *Kirchhoff-Institut für Physik, Universität Heidelberg, Heidelberg, Germany*[a]
[16] *Institute of Experimental Physics, Slovak Academy of Sciences, Košice, Slovak Republic*[f]
[17] *Department of Physics, University of Lancaster, Lancaster, UK*[b]
[18] *Department of Physics, University of Liverpool, Liverpool, UK*[b]
[19] *Queen Mary and Westfield College, London, UK*[b]
[20] *Physics Department, University of Lund, Lund, Sweden*[g]
[21] *CPPM, Aix-Marseille Université, CNRS/IN2P3, Marseille, France*
[22] *Departamento de Fisica Aplicada, CINVESTAV, Mérida, Yucatán, México*[j]
[23] *Departamento de Fisica, CINVESTAV IPN, México City, México*[j]
[24] *Institute for Theoretical and Experimental Physics, Moscow, Russia*[k]
[25] *Lebedev Physical Institute, Moscow, Russia*[e]
[26] *Max-Planck-Institut für Physik, München, Germany*
[27] *LAL, Université Paris-Sud, CNRS/IN2P3, Orsay, France*
[28] *LLR, Ecole Polytechnique, CNRS/IN2P3, Palaiseau, France*
[29] *LPNHE, Université Pierre et Marie Curie Paris 6, Université Denis Diderot Paris 7, CNRS/IN2P3, Paris, France*
[30] *Faculty of Science, University of Montenegro, Podgorica, Montenegro*[n]
[31] *Institute of Physics, Academy of Sciences of the Czech Republic, Praha, Czech Republic*[h]
[32] *Faculty of Mathematics and Physics, Charles University, Praha, Czech Republic*[h]
[33] *Dipartimento di Fisica Università di Roma Tre and INFN Roma 3, Roma, Italy*
[34] *Institute for Nuclear Research and Nuclear Energy, Sofia, Bulgaria*[e]
[35] *Institute of Physics and Technology of the Mongolian Academy of Sciences, Ulaanbaatar, Mongolia*
[36] *Paul Scherrer Institut, Villigen, Switzerland*
[37] *Fachbereich C, Universität Wuppertal, Wuppertal, Germany*
[38] *Yerevan Physics Institute, Yerevan, Armenia*
[39] *DESY, Zeuthen, Germany*
[40] *Institut für Teilchenphysik, ETH, Zürich, Switzerland*[i]
[41] *Physik-Institut der Universität Zürich, Zürich, Switzerland*[i]

[42] *Also at Physics Department, National Technical University, Zografou Campus, GR-15773 Athens, Greece*
[43] *Also at Rechenzentrum, Universität Wuppertal, Wuppertal, Germany*
[44] *Also at University of P.J. Šafárik, Košice, Slovak Republic*
[45] *Also at CERN, Geneva, Switzerland*
[46] *Also at Max-Planck-Institut für Physik, München, Germany*
[47] *Also at Comenius University, Bratislava, Slovak Republic*
[48] *Also at Faculty of Physics, University of Bucharest, Bucharest, Romania*
[49] *Also at Ulaanbaatar University, Ulaanbaatar, Mongolia*
[50] *Supported by the Initiative and Networking Fund of the Helmholtz Association (HGF) under the contract VH-NG-401.*

[51] *Absent on leave from NIPNE-HH, Bucharest, Romania*
[52] *On leave of absence at CERN, Geneva, Switzerland*
† *Deceased*

[a] *Supported by the Bundesministerium für Bildung und Forschung, FRG, under contract numbers 05H09GUF, 05H09VHC, 05H09VHF, 05H16PEA*
[b] *Supported by the UK Science and Technology Facilities Council, and formerly by the UK Particle Physics and Astronomy Research Council*
[c] *Supported by FNRS-FWO-Vlaanderen, IISN-IIKW and IWT and by Interuniversity Attraction Poles Programme, Belgian Science Policy*
[d] *Partially Supported by Polish Ministry of Science and Higher Education, grant DPN/N168/DESY/2009*
[e] *Supported by the Deutsche Forschungsgemeinschaft*
[f] *Supported by VEGA SR grant no. 2/7062/ 27*
[g] *Supported by the Swedish Natural Science Research Council*
[h] *Supported by the Ministry of Education of the Czech Republic under the projects LC527, INGO-LA09042 and MSM0021620859*
[i] *Supported by the Swiss National Science Foundation*
[j] *Supported by CONACYT, México, grant 48778-F*
[k] *Russian Foundation for Basic Research (RFBR), grant no 1329.2008.2*
[l] *This project is co-funded by the European Social Fund (75%) and National Resources (25%) - (EPEAEK II) - PYTHAGORAS II*
[m] *Supported by the Romanian National Authority for Scientific Research under the contract PN 09370101*
[n] *Partially Supported by Ministry of Science of Montenegro, no. 05-1/3-3352*

1 Introduction

The ep collisions at HERA provide a unique opportunity to search for new particles coupling directly to a lepton and a quark. An example of such particles are leptoquarks (LQs), colour triplet bosons which appear in a variety of beyond the Standard Model (SM) theories [1–4]. Particle interactions in the SM conserve lepton flavour. If this property is extended to LQ models any such particles produced at HERA would decay exclusively into a quark and a first generation lepton, namely an electron[1] or a neutrino. Searches for such signatures have previously been performed at HERA [5–7]. A dedicated analysis investigating the production of second and third generation leptoquarks has also been performed by the H1 Collaboration, where the final state contains a muon or the decay products of a tau lepton in combination with a hadronic system [8].

In this paper a search for leptoquarks coupling exclusively to a quark and a first generation lepton is performed using the full $e^{\pm}p$ collision data set taken in the years 1994-2007 by the H1 experiment at HERA. The data were recorded with an electron beam of energy 27.6 GeV, which was longitudinally polarised up to 38%, and a proton beam of energy up to 920 GeV, corresponding to a centre-of-mass energy $\sqrt{s}$ of up to 319 GeV. The total integrated luminosity of the analysed data is 446 pb^{-1}, which represents a factor of almost four increase with respect to the previously published H1 results. The presented results supersede those derived in previous searches for first generation leptoquarks by the H1 Collaboration [5].

2 Leptoquark Phenomenology and Standard Model Processes

2.1 Leptoquark production at HERA

The phenomenology of LQs at HERA is discussed in detail elsewhere [6]. The effective Lagrangian considered conserves lepton and baryon number, obeys the symmetries of the SM gauge groups $\mathrm{SU}(2)_L \times \mathrm{U}(1)_Y$ and $\mathrm{SU}(3)_C$ and includes both scalar and vector LQs. In the framework of the phenomenological Buchmüller-Rückl-Wyler (BRW) model [9], LQs are classified into 14 types [10] with respect to the quantum numbers spin J, weak isospin I and chirality C (left-handed L, right-handed R). Scalar ($J = 0$) LQs are denoted as S_I^C and vector ($J = 1$) LQs are denoted V_I^C in the following. LQs with identical quantum numbers except for weak hypercharge are distinguished using a tilde, for example V_0^R and $\tilde{V}_0^R$. Whereas all 14 LQs couple to electron-quark pairs, four of the left-handed LQs, namely S_0^L, S_1^L, V_0^L and V_1^L, may also decay to a neutrino-quark pair. In particular, for S_0^L and V_0^L the branching fraction of decays into an electron-quark pair is predicted by the model to be $\beta_e = \Gamma_{\mathrm{eq}}/(\Gamma_{\mathrm{eq}} + \Gamma_{\nu\mathrm{q}}) = 0.5$, where Γ_{eq} ($\Gamma_{\nu\mathrm{q}}$) denotes the partial width for the LQ decay to an electron (neutrino) and a quark q. The branching fraction of decays into a neutrino-quark pair is then given by $\beta_\nu = 1 - \beta_e$.

Leptoquarks carry both lepton (L) and baryon (B) quantum numbers. The fermion number $F = L + 3\,B$ is conserved. Leptoquark processes in ep collisions proceed directly via s-channel

[1] In this paper the term "electron" is used generically to refer to both electrons and positrons, if not otherwise stated.

resonant LQ production or indirectly via u-channel virtual LQ exchange. A dimensionless parameter λ defines the coupling at the lepton-quark-LQ vertex. For LQ masses M_{LQ} below $\sqrt{s}$, the s-channel production of $F = 2$ ($F = 0$) LQs dominates in e^-p (e^+p) collisions. For LQ masses above $\sqrt{s}$, both the s and u-channel, as well as the interference with SM processes, are important such that both e^-p and e^+p collisions have similar sensitivity to all LQ types.

2.2 Standard Model processes

The search reported here considers final states where the leptoquark decays into an electron and a quark or a neutrino and a quark. Such decays lead to topologies similar to those of deep-inelastic scattering (DIS) neutral current (NC) and charged current (CC) interactions at high negative four-momentum transfer squared Q^2. The analysis is therefore performed using event selections (see section 4.1) similar to those used in inclusive DIS analyses [11] and previous LQ searches [5].

The SM prediction for both NC and CC DIS processes is obtained using the Monte Carlo (MC) event generator DJANGOH [12], which is based on LEPTO [13] for the hard interaction and HERACLES [14] for leptonic single photon emission and virtual electroweak corrections. LEPTO combines $\mathcal{O}(\alpha_s)$ matrix elements with higher order QCD effects using the colour dipole model as implemented in ARIADNE [15]. The JETSET program [16] is used to simulate the hadronisation process. Additional SM background contributions from photoproduction processes are simulated using the PYTHIA [17] event generator, with the GRV-G LO [18] parameterisation of the photon parton density functions (PDFs). All SM expectations are based on the CTEQ6m [19] proton parton density function parameterisation, which includes only 12% of the H1 data analysed in this paper, in addition to 30 pb^{-1} of ZEUS data. At high Bjorken x, the CTEQ6m parameterisations are dominated by data from fixed target experiments due to the limited amount of HERA data included.

Generated events are passed through a GEANT [20] based simulation of the H1 apparatus, which takes into account the running conditions of the data taking. Simulated events are reconstructed and analysed using the same program chain as is used for the data.

3 Experimental Method

3.1 Data sets and lepton polarisation

The full H1 data sample is made up of 164 pb^{-1} recorded in e^-p collisions and 282 pb^{-1} in e^+p collisions, of which 35 pb^{-1} were recorded at $\sqrt{s} = 301$ GeV. Data collected from 2003 onwards were taken with a longitudinally polarised lepton beam. As leptoquarks are chiral particles, these data are analysed in separate polarisation samples, formed by combining all data periods with similar lepton beam polarisation $P_e = (N_R - N_L)/(N_R + N_L)$, where N_R (N_L) is the number of right- (left-) handed leptons in the beam. The average polarisation and luminosity of all data sets are detailed in table 1.

Collisions	$\sqrt{s}$ [GeV]	P_e [%]	$\mathcal{L}$ [pb^{-1}]
e^+p	301	0	35
e^-p	319	0	15
e^+p	319	0	67
e^+p	319	$+32$	98
e^+p	319	-38	82
e^-p	319	$+37$	46
e^-p	319	-26	103

Table 1: Centre-of-mass energy $\sqrt{s}$, average lepton beam polarisation P_e and integrated luminosity $\mathcal{L}$ of the analysed H1 data sets.

3.2 H1 detector

A detailed description of the H1 experiment can be found elsewhere [21]. Only the detector components relevant to this analysis are briefly described here. A right-handed Cartesian coordinate system is used with the origin at the nominal primary ep interaction vertex. The proton beam direction defines the positive z axis (forward direction). The polar angle θ and the transverse momenta P_T of all particles are defined with respect to this axis. The azimuthal angle ϕ defines the particle direction in the transverse plane.

The Liquid Argon (LAr) calorimeter [22] covers the polar angle range $4^\circ < \theta < 154^\circ$ with full azimuthal acceptance. The energies of electromagnetic showers are measured in the LAr calorimeter with a precision of $\sigma(E)/E \simeq 11\%/\sqrt{E/\text{GeV}} \oplus 1\%$ and hadronic energy deposits with $\sigma(E)/E \simeq 50\%/\sqrt{E/\text{GeV}} \oplus 2\%$, as determined in test beam measurements [23, 24]. A lead-scintillating fibre calorimeter[2] (SpaCal) [25] covering the backward region $153^\circ < \theta < 178^\circ$ completes the measurement of charged and neutral particles. The central ($20^\circ < \theta < 160^\circ$) and forward ($7^\circ < \theta < 25^\circ$) inner tracking detectors are used to measure charged particle trajectories and to reconstruct the interaction vertex. The measured trajectories fitted to the interaction vertex are referred to as tracks in the following. The LAr calorimeter and inner tracking detectors are enclosed in a superconducting magnetic coil with a field strength of 1.16 T. From the curvature of charged particle trajectories in the magnetic field, the central tracking system provides transverse momentum measurements with a resolution of $\sigma_{P_T}/P_T = 0.002P_T/\text{GeV} \oplus 0.015$. The return yoke of the magnetic coil is the outermost part of the detector and is equipped with streamer tubes forming the central muon detector ($4^\circ < \theta < 171^\circ$). In the very forward region of the detector ($3^\circ < \theta < 17^\circ$) a set of drift chambers detects muons and measures their momenta using an iron toroidal magnet. The luminosity is determined from the rate of the Bethe-Heitler process $ep \to ep\gamma$, measured using a photon detector located close to the beam pipe at $z = -103$ m, in the backward direction.

The LAr calorimeter provides the main trigger in this analysis [11]. In order to remove events induced by cosmic rays and other non-ep background, the event vertex is required to

[2]This device was installed in 1995, replacing a lead-scintillator sandwich calorimeter [21].

be reconstructed within ± 35 cm in z of the average nominal interaction point. In addition, topological filters and timing vetoes are applied.

3.3 Particle identification and event reconstruction

The scattered electron is identified as a compact and isolated cluster of energy in the electromagnetic part of the LAr calorimeter with an associated track in the inner tracking detectors. The hadronic final state is reconstructed using a particle flow algorithm to combine tracks and calorimeter deposits not associated to the scattered electron [26, 27]. The missing transverse momentum $P_T^{\rm miss}$, which may indicate the presence of neutrinos in the final state, is derived from all reconstructed particles in the event.

The kinematic quantities in NC events are determined using the electron method [28], which uses information exclusively from the scattered electron. In CC events, the kinematic quantities are determined exclusively from the hadronic final state [28]. The leptoquark mass $M_{\rm LQ} = \sqrt{Q^2/y}$ is reconstructed using the measured kinematics of the scattered electron (hadronic final state) in the analysis of NC (CC) topologies, where y is the inelasticity.

4 Data Analysis

4.1 DIS event selections

Neutral current events are selected by requiring a scattered electron with energy $E_e > 11$ GeV and $Q^2 > 133$ GeV^2. Additionally, a kinematic cut on the inelasticity $0.1 < y < 0.9$ is employed to remove regions of poor reconstruction, poor resolution, large QED radiative effects and background from photoproduction processes [5]. Background from neutral hadrons or photons misidentified as leptons is suppressed by requiring a charged track to be associated to the lepton candidate. Energy-momentum conservation requires that $\Sigma_i(E^i - P_z^i) = 2E_e^0$, where the sum runs over all reconstructed particles, P_z is the momentum along the proton beam axis and E_e^0 is the electron beam energy. Applying the condition $\Sigma_i(E^i - P_z^i) > 35$ GeV further suppresses the contamination from photoproduction background in which the scattered lepton is undetected in the backward direction and a hadron is misidentified as an electron. The $\Sigma_i(E^i - P_z^i)$ requirement also further suppresses the influence of radiative corrections arising from initial state bremsstrahlung.

Charged current events are selected by requiring significant missing transverse momentum, $P_T^{\rm miss} > 12$ GeV, which is due to the undetected neutrino. To ensure a high trigger efficiency and good kinematic resolution, the analysis is further restricted to the region $0.1 < y < 0.85$. The main SM background is due to photoproduction events, in which the scattered electron escapes undetected in the backward direction and transverse momentum is missing due to fluctuations in the detector response or undetected particles. This background is suppressed by exploiting the correlation between $P_T^{\rm miss}$ and the ratio $V_{\rm ap}/V_{\rm p}$ [6] of transverse energy flow anti-parallel and parallel to the hadronic final state transverse momentum vector [29].

4.2 Systematic uncertainties

The experimental systematic uncertainties included in the analysis of the polarised data taken in the years 2003-2007 are described in the following. The systematic uncertainties on the 1994-2000 data are described in the previous H1 publication [5].

In the NC event samples, a systematic scale uncertainty of 1-3% is assigned to the electromagnetic energy measured in the LAr calorimeter, depending on the z-coordinate of the impact position of the scattered electron. A 0.5% component of this uncertainty is considered as correlated. In addition, an uncorrelated uncertainty on the polar angle measurement of the scattered lepton of 2 mrad for $\theta_e > 120^\circ$ and 3 mrad elsewhere is also included.

An uncertainty of 2% is assigned to the scale of the measured hadronic energy for events in the CC event samples, of which 1% is considered to be a correlated component. In addition, a 10% correlated uncertainty is assigned to the amount of energy in the LAr calorimeter attributed to noise for events in the CC event samples.

Other experimental systematic uncertainties are found to have a negligible impact on the analysis. The effect of the above systematic uncertainties on the SM expectation is determined by varying the experimental quantities by ± 1 standard deviation in the MC samples and propagating these variations through the whole analysis.

The luminosity measurement has an average uncertainty of 3%. The uncertainty on the polarisation measurement is 3.5% and is found to have a negligible effect on the limit calculations performed in section 5.3.

All data sets are compared to a SM prediction based on the CTEQ6m [19] parameterisation of the parton densities inside the proton. The uncertainties of this parameterisation are propagated through the analysis using the full set of eigenvector PDFs, and the effect is added in quadrature to the experimental uncertainties listed above.

5 Results

5.1 Mass distributions

Mass spectra of the four H1 data sets taken with a longitudinally polarised lepton beam as defined in table 1 are shown in figure 1, where both the NC and CC event samples are presented. The mass spectra of the complete electron and positron H1 data sets are presented in figure 2. A good description of the H1 data by the SM is observed, where the expectation is dominated by DIS processes in all event samples, with small additional contributions from photoproduction. Since no evidence for LQ production is observed in any of the NC or CC data samples, the data are used to set constraints on LQs coupling to first generation fermions.

5.2 Statistical Method

For the limit analysis, the data are studied in bins in the $M_{LQ} - y$ plane, where the NC and CC data samples with different lepton beam charge and polarisation are kept as distinct data sets. In total, $N_{\rm bin} = 1408$ bins are considered, divided equally between the NC and CC event samples. For a given bin i, the predicted LQ signal contribution is denoted s_i and the predicted number of events in the absence of a LQ signal is denoted b_i. The number of events in the presence of a LQ signal is thus $s_i + b_i$ and is obtained as a function of the LQ mass and coupling by a reweighting procedure [5]. The limits are determined from a statistical analysis which uses the method of fractional event counting, optimised for the presence of systematic uncertainties [30]. For a given leptoquark type, mass and coupling hypothesis, a test statistic X is constructed as a fractional event count of all events:

$$X \;=\; \sum_{i=1}^{N_{\rm bin}} w_i n_i \,, \tag{1}$$

where the sum runs over all bins and n_i is the number of events observed in bin i. The weights w_i are chosen such that in the presence of a LQ signal the test statistic X is larger than that expected from the SM. In particular, bins with a large and positive s_i have weights close to one, whereas bins with s_i close to zero have weights close to zero. If s_i is negative in a given bin due to interference effects, the corresponding bin weight is also negative. This has the desired effect that an event deficit in such a bin still leads to a X larger than the SM expectation and thus is interpreted correctly as a signal contribution. The presence of systematic uncertainties may reduce the sensitivity of a given bin. The weight is therefore defined in such a way as to ensure that only bins with both a large signal contribution and small systematic uncertainties enter with sizeable weights into the test statistic X. This is achieved by defining the weights as solutions of the following set of linear equations [30]:

$$s_i = k_1 \left[(s_i + b_i) w_i + \sum_j V_{ij}^{SB} w_j \right] + k_2 \left[b_i w_i + \sum_j V_{ij}^{B} w_j \right] \,. \tag{2}$$

In this analysis, the constants k_1 and k_2 are set to one, which is the appropriate choice for testing signals with a well defined cross section prediction [30]. The covariance matrices of all bins in the presence (absence) of the LQ signal, V_{ij}^{SB} (V_{ij}^{B}), are calculated as:

$$V_{ij}^{SB} = \sum_{k=1}^{N_{\rm sys}} \sigma_{ki}^{SB} \sigma_{kj}^{SB} \quad \text{and} \quad V_{ij}^{B} = \sum_{k=1}^{N_{\rm sys}} \sigma_{ki}^{B} \sigma_{kj}^{B} \,, \tag{3}$$

where σ_{ki}^{SB} (σ_{ki}^{B}) are the one sigma shifts induced from systematic source k to the number of events expected in bin i in the presence (absence) of the LQ signal. The sums run over the $N_{\rm sys}$ sources of systematic uncertainty. In the case of negligible systematic uncertainties, equation 3 is equivalent to the weight definition used in [5].

Limits are obtained by performing a frequentist analysis of the test statistic obtained from the data, $X^{\rm data}$. For each signal hypothesis, a large number of MC experiments, typically $\mathcal{O}(10^5)$, are generated by varying the expected number of events $s_i + b_i$ within the uncertainties.

Systematic uncertainties are treated as Gaussian distributions and statistical fluctuations are simulated using Poisson statistics. For each MC experiment e, a test statistic X^e is calculated. A probability $p^{\rm data}$ is calculated as the fraction of MC experiments which have $X^e < X^{\rm data}$. The LQ hypothesis is excluded at a given confidence level (CL) if $p^{\rm data} < 1-{\rm CL}$. In addition to this condition, a power constraint is applied [31]. The power constraint avoids the exclusion of LQ signals beyond the sensitivity of the experiment, which may otherwise occur due to statistical fluctuations in the data in the opposite direction to that expected from the LQ hypothesis. A probability $p^{1\sigma}$ is determined as the fraction of MC experiments with $X^e < X^{1\sigma}$. Here, $X^{1\sigma}$ is the value of the test statistic which corresponds to a 1σ downwards fluctuation of the SM. It is determined from a second set of MC experiments, where each experiment $\tilde{e}$ is simulated in the absence of a LQ signal, that is by simulating systematic and statistical fluctuations of b_i. The value $X^{1\sigma}$ is determined such that the fraction of MC experiments with $X^{\tilde{e}} < X^{1\sigma}$ is equal to the single-sided 1σ quantile, 15.9%. LQ models are excluded at 95% CL with the power constraint applied, if both $p^{\rm data}$ and $p^{1\sigma}$ are below 0.05.

5.3 Limits

Exclusion limits are first derived within the phenomenological BRW model [9] described in section 2.1. Upper limits on the coupling λ obtained at 95% CL are shown as a function of the leptoquark mass in figure 3, displayed as groups of scalar and vector LQs for both $F = 2$ and $F = 0$. The presented limits extend beyond those from previous leptoquark and contact interaction analyses based on smaller HERA data sets by the H1 [5, 32] and ZEUS [7, 33] collaborations. For a coupling of electromagnetic strength $\lambda = \sqrt{4\pi\alpha_{\rm em}} = 0.3$, LQs produced in ep collisions decaying to an electron-quark or a neutrino-quark pair are excluded at 95% CL up to leptoquark masses between 277 GeV (V_0^R) and 800 GeV (V_0^L), depending on the leptoquark type.

Within the framework of the BRW model, the $\tilde{S}^L_{1/2}$ LQ decays exclusively to an electron-quark pair, resulting in a branching fraction for decays into charged leptons of $\beta_e = 1.0$, whereas the S^L_0 LQ also decays to neutrino-quark, resulting in $\beta_e = 0.5$. The H1 limits on $\tilde{S}^L_{1/2}$ and S^L_0 presented in this paper are compared to those from other experiments in figure 4. Limits from the previous H1 publication [5] are also shown. Indirect limits from searches for new physics in e^+e^- collisions at LEP by the OPAL [34] and L3 [35] experiments are indicated, as well as the limits from DØ [36,37] at the Tevatron and from the CMS [38,39] and ATLAS [40] experiments at the LHC. The limits from hadron colliders are based on searches for LQ pair-production and are independent of the coupling λ, where the strongest current limit for $\beta_e = 1.0$ ($\beta_e = 0.5$) scalar LQs is 384 GeV (340 GeV) as reported by the CMS collaboration. For these leptoquark masses, this analysis rules out the $\tilde{S}^L_{1/2}$ and S^L_0 LQs for coupling strengths larger than 0.64 and 0.14 respectively. The H1 limits at high leptoquark mass values are also compared with those obtained in a contact interaction analysis [41], which is based on single differential NC cross sections ${\rm d}\sigma/{\rm d}Q^2$ measured using the same data. The additional impact of the CC data can be seen in the case of the S^L_0 LQ, where a stronger limit is achieved in this analysis, whereas for the $\tilde{S}^L_{1/2}$ LQ the two analyses result in a similar limit.

Signatures similar to those expected from LQ decays also appear in supersymmetric models with R-parity violation [42]. In such models, the production and direct decay of the $\tilde{u}^j_L$ ($\tilde{d}^k_R$)

squark via a λ'_{1j1} (λ'_{11k}) coupling is equivalent to the interaction of the $\tilde{S}^L_{1/2}$ (S^L_0) LQ with a lepton-quark pair, and as such the results described in the previous paragraph are also valid for these squark types, assuming the direct decay dominates. More general limits on squark production with R-parity violating decays are presented in a dedicated H1 publication [43].

Beyond the BRW ansatz, β_e may be considered as a free parameter and the couplings and therefore also the branching ratios to electron-quark and neutrino-quark are not necessarily equal. By investigating such a model, mass dependent constraints on the LQ branching ratio β_e can be set for a given value of the electron-quark-LQ coupling λ_e. Excluded regions in the β_e–M_{LQ} plane for three different coupling strengths are shown for a vector LQ with quantum numbers identical to V^L_0 in figure 5(a) and for a scalar LQ with quantum numbers identical to S^L_0 in figure 5(b). Similar exclusion limits from the Tevatron (DØ [36, 37]) and the LHC (CMS [39] and ATLAS [40]), which do not depend on λ_e, are also shown in figure 5. For an electron-quark-LQ coupling of electromagnetic strength $\lambda_e = 0.3$ the H1 limits extend to high leptoquark masses beyond the kinematic limit of resonant LQ production, and for most values of β_e extend considerably beyond the region currently excluded by hadron colliders.

6 Summary

A search for first generation scalar and vector leptoquarks is performed using the complete H1 $e^{\pm}p$ data taken at a centre-of-mass energy of up to $319\,\mathrm{GeV}$ and corresponding to an integrated luminosity of $446\ \mathrm{pb}^{-1}$. The H1 data are well described by the SM prediction and no leptoquark signal is observed. Limits are derived on 14 leptoquark types and assuming a coupling strength of $\lambda = 0.3$ leptoquarks are ruled out up to masses of 800 GeV, which is beyond the current limits from hadron colliders.

Acknowledgements

We are grateful to the HERA machine group whose outstanding efforts have made this experiment possible. We thank the engineers and technicians for their work in constructing and maintaining the H1 detector, our funding agencies for financial support, the DESY technical staff for continual assistance and the DESY directorate for support and for the hospitality which they extend to the non-DESY members of the collaboration.

References

[1] J. C. Pati and A. Salam, Phys. Rev. **D10** (1974) 275;
H. Georgi and S. L. Glashow, Phys. Rev. Lett. **32** (1974) 438;
P. Langacker, Phys. Rept. **72** (1981) 185.

[2] B. Schrempp and F. Schrempp, Phys. Lett. **B153** (1985) 101;
J. Wudka, Phys. Lett. **B167** (1986) 337.

[3] S. Dimopoulos and L. Susskind, Nucl. Phys. **B155** (1979) 237;
S. Dimopoulos, Nucl. Phys. **B168** (1980) 69;
E. Farhi and L. Susskind, Phys. Rev. **D20** (1979) 3404;
E. Farhi and L. Susskind, Phys. Rept. **74** (1981) 277.

[4] H. P. Nilles, Phys. Rept. **110** (1984) 1;
H. E. Haber and G. L. Kane, Phys. Rept. **117** (1985) 75.

[5] A. Aktas *et al.* [H1 Collaboration], Phys. Lett. **B629** (2005) 9 [hep-ex/0506044].

[6] C. Adloff *et al.* [H1 Collaboration], Eur. Phys. J. **C11** (1999) 447 [Erratum ibid. **C14** (2000) 553] [hep-ex/9907002].

[7] S. Chekanov *et al.* [ZEUS Collaboration], Phys. Rev. **D68** (2003) 052004 [hep-ex/0304008].

[8] F. D. Aaron *et al.* [H1 Collaboration], Phys. Lett. **B701** (2011) 20 [arXiv:1103.4938].

[9] W. Buchmüller, R. Rückl and D. Wyler, Phys. Lett. **B191** (1987) 442 [Erratum ibid. **B448** (1999) 320].

[10] B. Schrempp, proceedings of the workshop "Physics at HERA", vol. 2, eds. W. Buchmüller and G. Ingelman, DESY (1991), p. 1034.

[11] C. Adloff *et al.* [H1 Collaboration], Eur. Phys. J. **C30** (2003) 1 [hep-ex/0304003].

[12] G. A. Schuler and H. Spiesberger, DJANGOH version 4.1, proceedings of the workshop "Physics at HERA", vol. 3, eds. W. Buchmüller, G. Ingelman, DESY (1992), p. 1419.

[13] G. Ingelman, proceedings of the workshop "Physics at HERA", vol. 3, eds. W. Buchmüller, G. Ingelman, DESY (1992), p. 1366.

[14] A. Kwiatkowski, H. Spiesberger and H.-J. Möhring, Comput. Phys. Commun. **69** (1992) 155.

[15] L. Lönnblad, Comput. Phys. Commun. **71** (1992) 15.

[16] T. Sjöstrand and M. Bengtsson, Comput. Phys. Commun. **43** (1987) 367.

[17] T. Sjöstrand *et al.*, PYTHIA version 6.1, Comput. Phys. Commun. **135** (2001) 238 [hep-ph/0010017].

[18] M. Glück, E. Reya and A. Vogt, Phys. Rev. **D46** (1992) 1973.

[19] J. Pumplin *et al.* [CTEQ Collaboration], JHEP **0207** (2002) 012 [hep-ph/0201195].

[20] R. Brun *et al.*, "GEANT 3 User's Guide", CERN-DD/EE-84-1 (1987).

[21] I. Abt *et al.* [H1 Collaboration], Nucl. Instrum. Meth. **A386** (1997) 310;
I. Abt *et al.* [H1 Collaboration], Nucl. Instrum. Meth. **A386** (1997) 348.

[22] B. Andrieu *et al.* [H1 Calorimeter Group], Nucl. Instrum. Meth. **A336** (1993) 460.

[23] B. Andrieu *et al.* [H1 Calorimeter Group], Nucl. Instrum. Meth. **A336** (1993) 499.

[24] B. Andrieu *et al.* [H1 Calorimeter Group], Nucl. Instrum. Meth. **A350** (1994) 57.

[25] R.-D. Appuhn *et al.* [H1 SpaCal Group], Nucl. Instrum. Meth. **A386** (1997) 397.

[26] B. Portheault, "Première mesure des sections efficaces de courant chargé et neutre avec le faisceau de positrons polarisé à HERA II et analyses QCD-électrofaibles", Ph.D. thesis, Université Paris XI (2005), LAL-05-05, available at `http://www-h1.desy.de/publications/theses_list.html`.

[27] R. Kogler, "Measurement of jet production in deep-inelastic ep scattering at HERA", Ph.D. thesis, Universität Hamburg (2011), MPP-2010-175, available at `http://www-h1.desy.de/publications/theses_list.html`.

[28] F. Jacquet and A. Blondel, proceedings of "Study of an ep facility for Europe", ed. U. Amaldi, DESY (1979), DESY 79/48, p. 391.

[29] R. Plačakytė, "First measurement of charged current cross sections with longitudinally polarised positrons at HERA", Ph.D. thesis, Max-Planck-Institut für Physik, Munich (2006), available at `http://www-h1.desy.de/publications/theses_list.html`.

[30] P. Bock, JHEP **0701** (2007) 080 [hep-ex/0405072].

[31] G. Cowan, K. Cranmer, E. Gross and O. Vitells, arXiv:1105.3166.

[32] C. Adloff *et al.* [H1 Collaboration], Phys. Lett. **B568** (2003) 35 [hep-ex/0305015].

[33] S. Chekanov *et al.* [ZEUS Collaboration], Phys. Lett. **B591** (2004) 23 [hep-ex/0401009].

[34] G. Abbiendi *et al.* [OPAL Collaboration], Eur. Phys. J. **C6** (1999) 1 [hep-ex/9808023].

[35] M. Acciarri *et al.* [L3 Collaboration], Phys. Lett. **B489** (2000) 81 [hep-ex/0005028].

[36] V. M. Abazov *et al.* [DØ Collaboration], Phys. Lett. **B681** (2009) 224 [arXiv:0907.1048].

[37] V. M. Abazov *et al.* [DØ Collaboration], arXiv:1107.1849.

[38] V. Khachatryan *et al.* [CMS Collaboration], Phys. Rev. Lett. **106** (2011) 201802 [arXiv:1012.4031].

[39] S. Chatrchyan *et al.* [CMS Collaboration], Phys. Lett. **B703** (2011) 246 [arXiv:1105.5237].

[40] G. Aad *et al.* [ATLAS Collaboration], Phys. Rev. **D83** (2011) 112006 [arXiv:1104.4481].

[41] F. D. Aaron *et al.* [H1 Collaboration], arXiv:1107.2478.

[42] J. Butterworth and H. K. Dreiner, Nucl. Phys. **B397** (1993) 3 [hep-ph/9211204].

[43] F. D. Aaron *et al.* [H1 Collaboration], Eur. Phys. J. **C71** (2011) 1572 [arXiv:1011.6359].

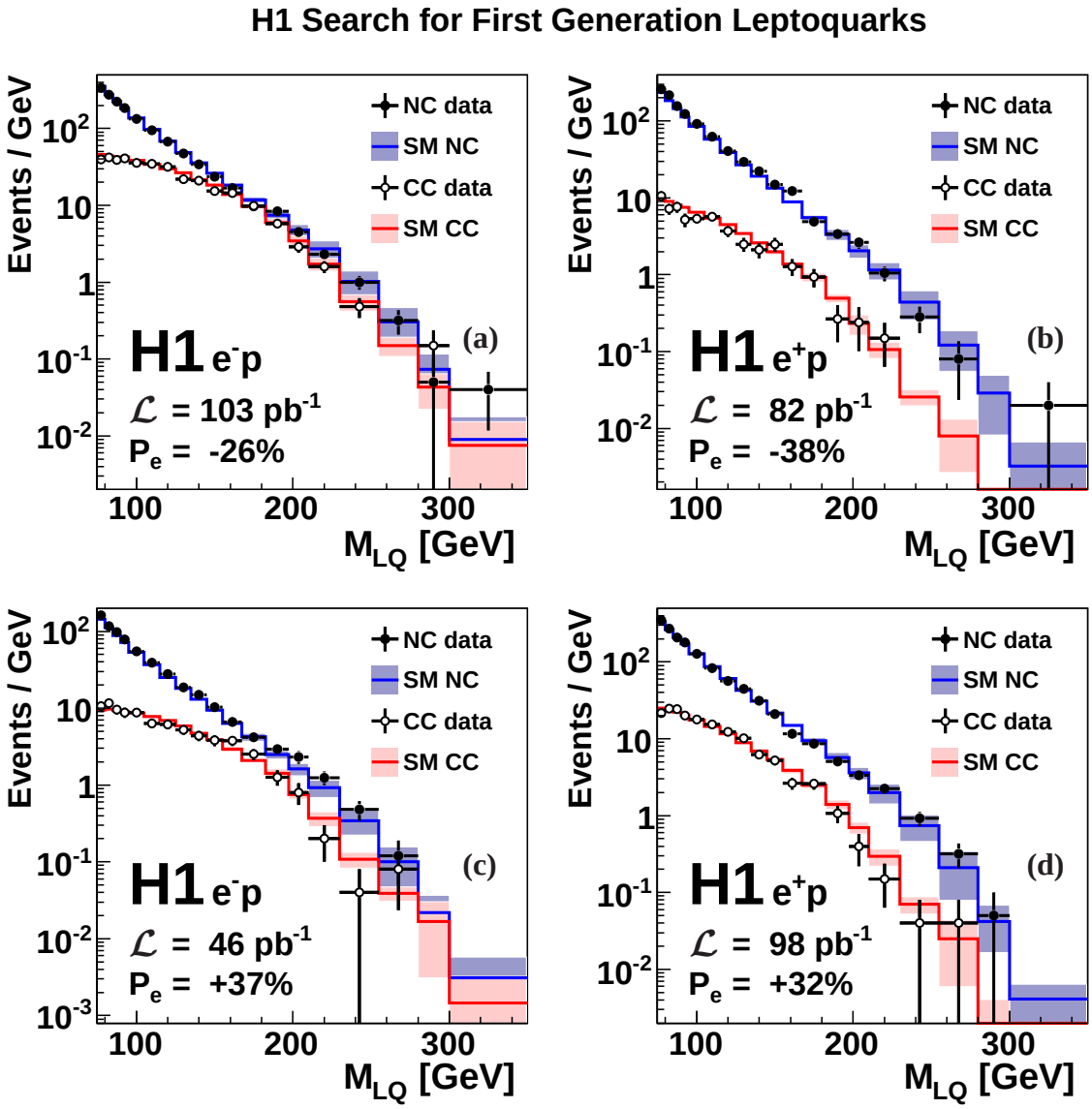

Figure 1: The reconstructed leptoquark mass in the search for first generation leptoquarks in the 2003-2007 H1 data, which was taken with a polarised lepton beam. The left-handed electron data (a) and left-handed positron data (b) are shown in the top row; the right-handed electron data (c) and right-handed positron data (d) are shown in the bottom row. The luminosity $\mathcal{L}$ and average longitudinal lepton polarisation P_e of each data set is indicated. The NC (solid points) and CC (open points) data are compared to the SM predictions (histograms), where the shaded bands indicate the total SM uncertainties.

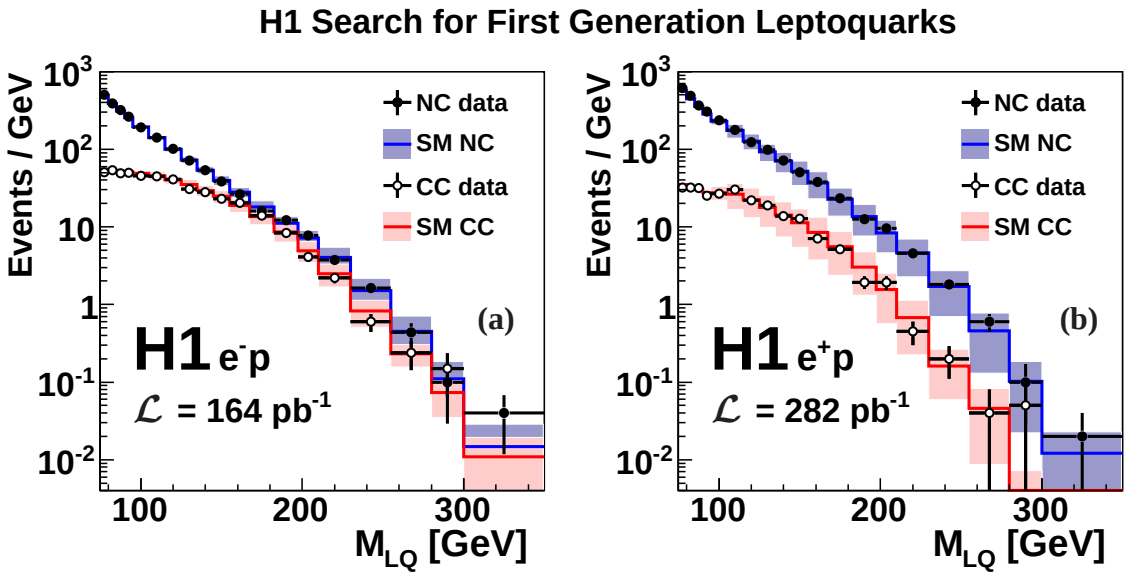

Figure 2: The reconstructed leptoquark mass in the search for first generation leptoquarks in the full H1 electron (a) and positron (b) data. The luminosity $\mathcal{L}$ of each data set is indicated. The NC (solid points) and CC (open points) data are compared to the SM predictions (histograms), where the shaded bands indicate the total SM uncertainties.

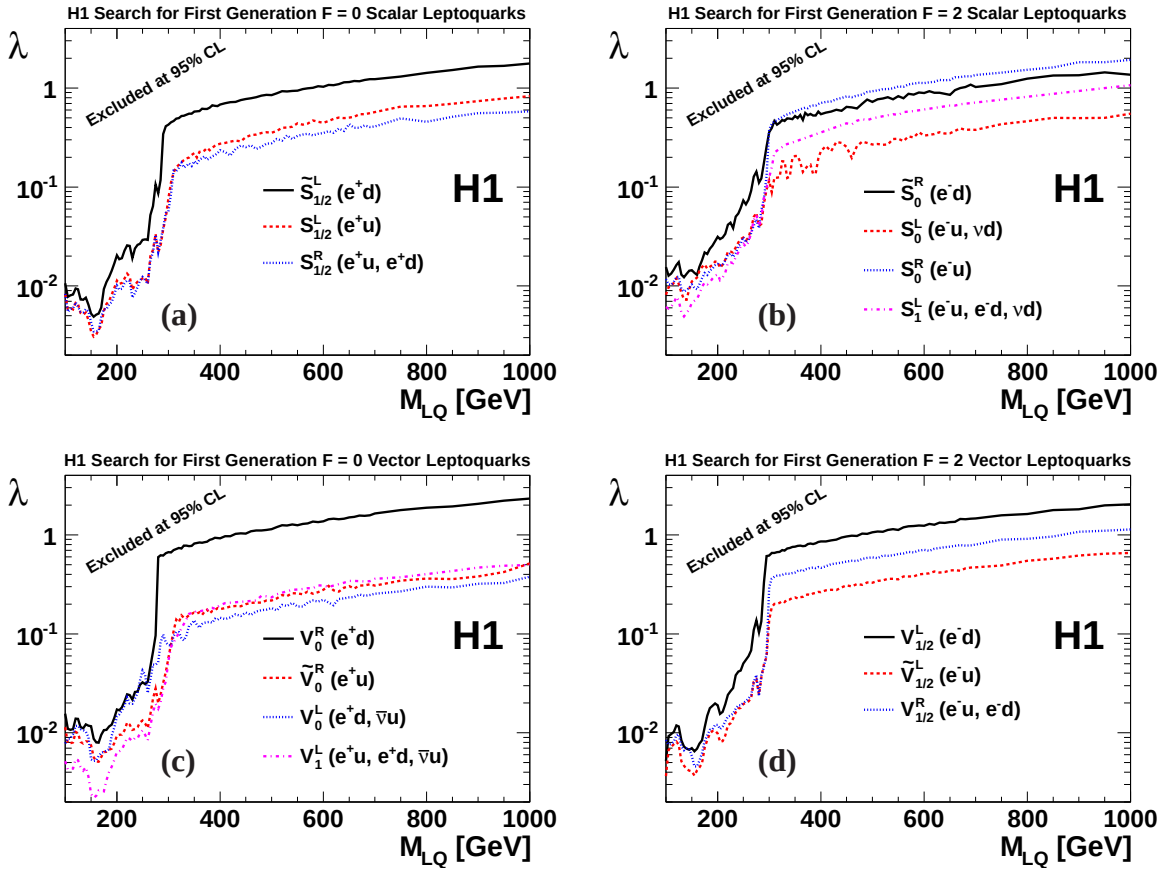

Figure 3: Exclusion limits for the 14 leptoquarks (LQs) described by the Buchmüller, Rückl and Wyler (BRW) model. The limits are expressed on the coupling λ as a function of leptoquark mass for the scalar LQs with $F = 0$ (a) and $F = 2$ (b) and the vector LQs with $F = 0$ (c) and $F = 2$ (d). Domains above the curves are excluded at $95\%\,\mathrm{CL}$. The parentheses after the LQ name indicate the fermion pairs coupling to the LQ, where pairs involving anti-quarks are not shown.

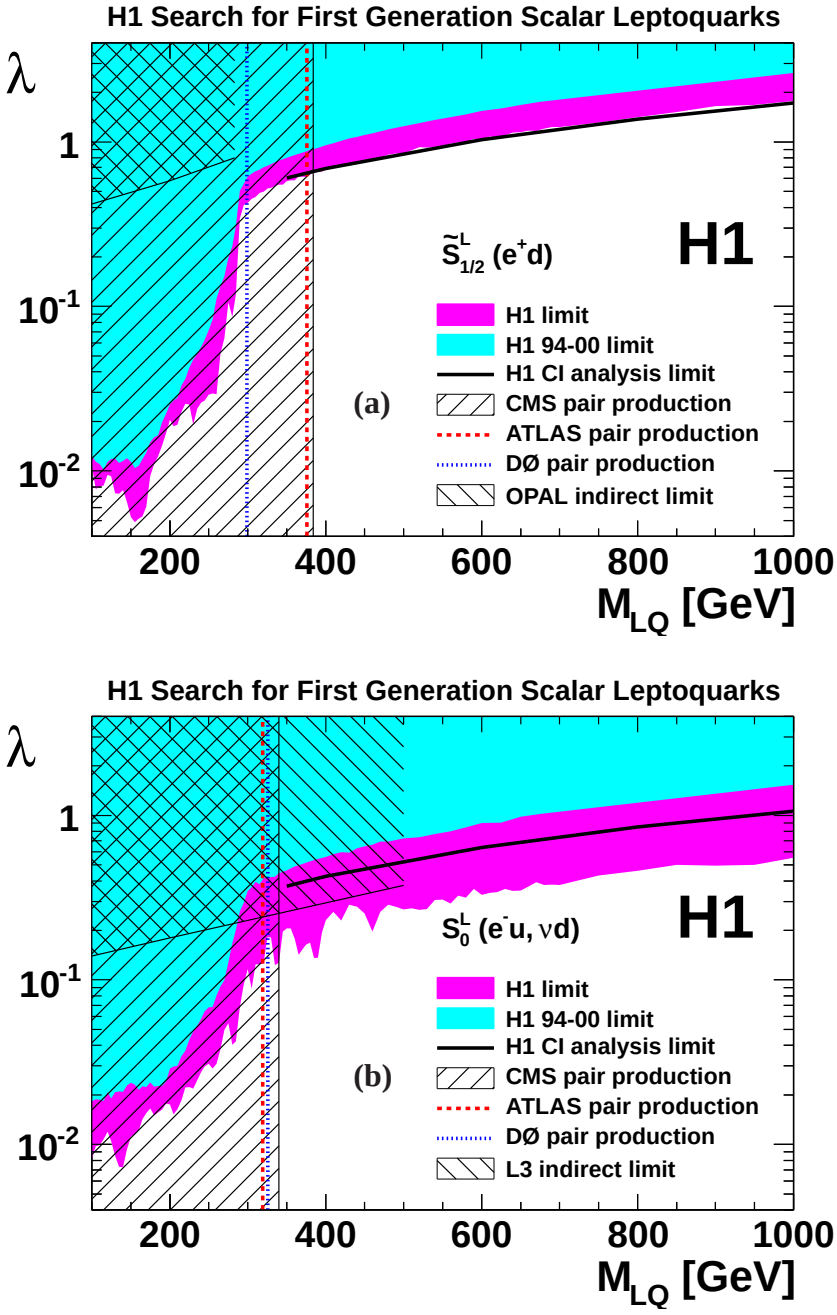

Figure 4: Exclusion limits on the coupling λ as a function of the leptoquark mass for the $\tilde{S}^L_{1/2}$ (a) and S^L_0 (b) leptoquarks in the framework of the BRW model. The parentheses after the LQ name indicate the fermion pairs coupling to the LQ, where pairs involving anti-quarks are not shown. Domains above the curves are excluded at 95% CL. Limits from the previous H1 publication (94-00) are also indicated. For comparison, limits from LEP (OPAL and L3), the Tevatron (DØ) and the LHC (CMS and ATLAS, $\sqrt{s} = 7$ TeV data) are shown for comparison, as well as constraints on LQs with masses above 350 GeV from the H1 contact interaction (CI) analysis.

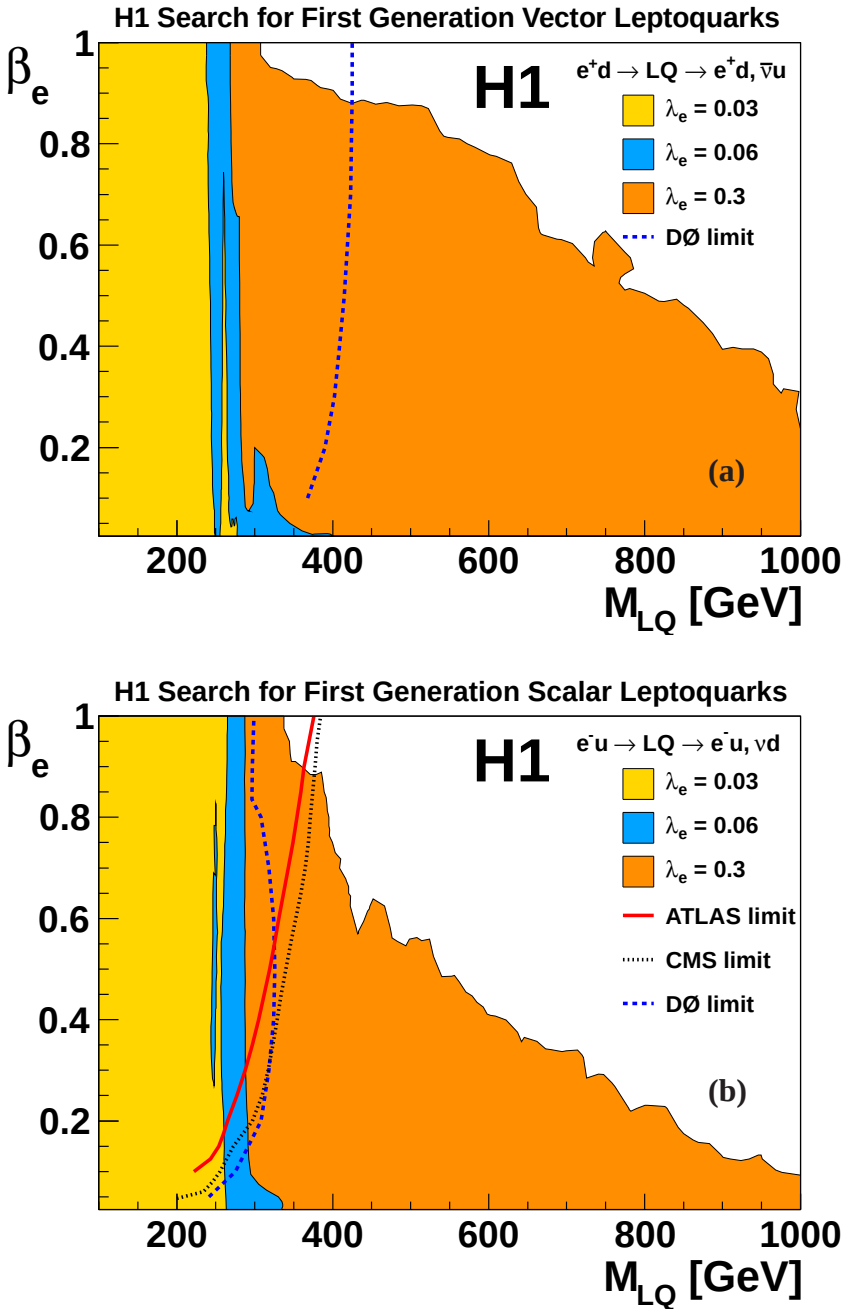

Figure 5: Regions of β_e–M_{LQ} ruled out by the combination of the NC and CC analyses for (a) a vector LQ coupling to e^+d (with the quantum numbers of the V_0^L) and (b) for a scalar LQ coupling to e^-u (with the quantum numbers of the S_0^L), where only LQ decays into eq and νq are considered. Excluded regions at 95% CL are shown as the coloured areas for three different values of the electron-quark-LQ coupling λ_e. Limits from the Tevatron (DØ) and the LHC (CMS and ATLAS, $\sqrt{s} = 7$ TeV data), which do not depend on λ_e, are also indicated.